

# Effect of Biofilms on Crevice Corrosion of Stainless Steels in Coastal Seawater

H.-J. Zhang and S.C. Dexter\*

## ABSTRACT

The effect of biofilms on crevice corrosion of stainless steels (SS) UNS S31603 (type 316L SS), S31725 (type 317LM SS), N08904 (type 904L SS), and N08367 (6XN) in coastal seawater was investigated using the remote crevice assembly technique. One set of naturally initiated tests and one set of preinitiated tests were performed. For UNS N08367, anodes in natural initiation tests did not corrode, while preinitiated corrosion did not propagate in natural or control seawater. Biofilms did not significantly affect initiation times for UNS S31603 and S31725, while for the corroded samples of UNS N08904, biofilms significantly decreased crevice corrosion initiation times. Biofilms greatly increased the propagation rate for UNS S31603, S31725, and N08904, as measured by maximum and average depths of attack, weight loss, and current density. Theoretical weight losses ( $W_{-}$ ) calculated using Faraday's law and the measured current densities were in good agreement with the measured weight losses ( $W_m$ ). For anodes in preinitiated tests, current densities calculated from cathodic polarization curves also were in good agreement with the measured current densities. The increased propagation rate of crevice corrosion was caused by an increase in the cathodic reaction rate, which was due to the action of biofilms. Effective control conditions were achieved in the long-term tests by a

combination of heat treating the water at 80°C before exposure and periodically exchanging the cathode panels after 1 h of immersion in fresh water at 60°C.

**KEY WORDS:** bacteria, biofilm, cathodic polarization, crevice corrosion, current density, initiation, propagation, seawater, stainless steel, weight loss

## INTRODUCTION

Biofilms can shift the open-circuit potential ( $E_{\text{corr}}$ ) of stainless steels (SS) in the noble direction in seawater,<sup>1-6</sup> brackish water,<sup>7-8</sup> and fresh water.<sup>7-8</sup> Biofilms are the thin, distributed films formed by microorganisms such as bacteria and algae and their associated expolymers. There has been much speculation about the effect of  $E_{\text{corr}}$  ennoblement on the initiation and propagation of pitting and crevice corrosion.<sup>1-8</sup> Zhang and Dexter suggested the biological effect may be more significant for such alloys as UNS N08904<sup>(1)</sup> (type 904L SS), which has intermediate resistance to crevice corrosion, than for highly resistant alloys (such as UNS N08367 [6XN]) or low-resistance alloys (such as UNS S30400 [type 304 SS] and S31603 [type 316L SS]).<sup>9</sup> Johnsen and Bardal pointed out that  $E_{\text{corr}}$  ennoblement should decrease the initiation time for crevice corrosion and pitting.<sup>4</sup> Likewise, Scotto, et al., suggested that an increase in the oxygen (O) reduction rate by bacteria at the cathode surface should increase the localized corrosion of passive metals in natural seawater.<sup>6</sup> Dexter, et al., showed that bacteria in the crevice solution could contribute to the depletion of O,

Submitted for publication March 1993; in revised form, July 1994. Presented as paper no. 400 at CORROSION/92, April 1992, Nashville, TN, and at the 12th International Corrosion Congress, Houston, TX, September 1993.

\* University of Delaware, College of Marine Studies, Lewes, DE, 19958.

<sup>(1)</sup> UNS numbers are listed in *Metals and Alloys in the Unified Numbering System*, published by the Society of Automotive Engineers (SAE) and cosponsored by ASTM.

potentially decreasing initiation times for crevice corrosion.<sup>10</sup>

Kain and Lee studied crevice corrosion of UNS S31600 and N08904 in natural and artificial seawaters using the remote crevice assembly technique.<sup>11</sup> They found that for UNS S31600, the initiation times in natural and artificial seawater were almost the same, while the corrosion current in natural seawater was one order of magnitude higher than that in artificial seawater. For UNS N08904, the initiation time in natural seawater was 10% that in artificial seawater, and the corrosion current in natural seawater was two orders of magnitude higher than that in artificial seawater. Kain and Lee also found that increasing the temperature of natural seawater from 30°C to 50°C decreased the corrosion current for UNS N08904 nearly three orders of magnitude. It was concluded that the biological species in natural seawater caused the increase in the crevice corrosion, but no biological analysis was done.

Valen also used a remote crevice assembly device to study the crevice corrosion of UNS S31603 in natural and artificial seawaters.<sup>12</sup> He found that the initiation time for UNS S31603 in natural seawater was slightly longer than that in artificial seawater and that the current density for UNS S31603 in natural seawater was one to two orders of magnitude higher than that in artificial seawater, despite a cathode-to-anode area ratio that was 20 to 400 times larger in artificial seawater than in natural seawater.

Mollica, et al., studied the effect of temperature on the crevice corrosion of SS in natural seawater.<sup>13</sup> They immersed the crevice samples in four tanks at temperatures of 25°C, 30°C, 35°C, and 40°C. Results showed that, as the temperature increased from 25°C to 40°C, the initiation probability and the propagation rate of crevice corrosion decreased for the alloys that had intermediate resistance to crevice corrosion. However, for alloys that had low resistance (e.g., UNS S31600), the initiation probability and propagation rate remained unchanged. The investigators attributed the decreased propagation rate for the alloys that had intermediate resistance to a decrease in the activity of aerobic bacteria at 40°C, but they did not analyze the bacteria on the sample surfaces.

Gallagher, et al., studied crevice corrosion of SS in natural, transported, and artificial seawaters using a multiple crevice assembly device.<sup>14</sup> They found that for a range of alloys, including UNS S31603 and N08904, crevice corrosion was dramatically less in artificial seawater than in natural and transported seawaters. However, they did not give information about crevice corrosion initiation times. They

attributed the high rate of crevice corrosion in these seawaters to the organisms on the samples. However, no analysis of the organisms was made.<sup>14</sup>

Preliminary work by Zhang and Dexter found that biofilms tended to decrease the initiation times for crevice corrosion on UNS S30400, S31603, S31725 (type 317LM SS), and N08904.<sup>9</sup> Biofilms had little effect on the propagation of crevice corrosion on UNS S30400 and S31603, which have low resistance, but had considerable effects on propagation on UNS S31725 and N08904, which have intermediate resistance. To do experiments in a control water that had the same chemistry but few bacteria, Zhang and Dexter used filtered natural seawater (0.2 µm mesh) rather than artificial seawater. This provided effective control conditions for only ~ 500 h. They suggested that more effective control methods were needed for long-term tests.

The present work was undertaken to present data about the effect of marine biofilms on the crevice corrosion of SS in tests using a more effective control method than the filtering technique used by Zhang and Dexter.<sup>9</sup> This more effective method combined pasteurization of natural coastal seawater at 80°C for 4 h with periodic replacement of cathodes. The work also was done to present data about the effect of biofilms on propagation of crevice corrosion when using preinitiated anodes and pre-nobled cathodes to eliminate the initiation step in crevice corrosion.

UNS S31603 was selected because of its low resistance to crevice corrosion in seawater. UNS S31725 and N08904 were used as examples of newer alloys that had intermediate resistance in seawater, and UNS N08367, which contains 6% molybdenum (Mo), was used as a highly resistant control for comparison.

## EXPERIMENTAL

Nominal compositions of the SS used are shown in Table 1. Annular electrodes (31.7 mm outer diam, 9.6 mm inner diam, 3.0 mm thickness) were used as anodes. Large panels of the same alloys (152 mm by 101 mm by 2 mm) were used as cathodes. Samples were prepared before testing by surface grinding through 320-grit silicon carbide paper, degreasing with soap and water, and rinsing in milli-Q water (Millipore<sup>†</sup>).

Coastal seawater was obtained from the tidal part of the Broadkill River where it enters the lower Delaware Bay. This water had the following characteristics: temperature, 22°C to 26°C; salinity, 25 to 31 parts per thousand (ppt); O<sub>2</sub>, air saturated (5 ppm to 8 ppm); and pH 7.7 to 8.1. These values varied daily with tidal cycle and fresh water run-off. The water was brought to the lab, where the tests were

<sup>†</sup> Trade name.

**TABLE 1**  
Nominal Compositions of SS (wt%)(<sup>A</sup>)

Alloy	Cr	Ni	Mo	Cu	C	Si	Mn	S	P	N	Co
UNS S31603	16.23	10.11	2.10	0.36	0.022	0.43	1.84	0.001	0.034	0.04	0.22
UNS S31725	18.29	16.27	4.36	0.17	0.024	0.48	1.66	0.025	0.020	0.09	0.31
UNS N08904	19.00	24.30	4.28	1.38	0.012	0.36	1.59	0.0003	0.019	0.06	0.29
UNS N08367	20.28	23.82	6.22	0.30	0.018	0.49	0.36	0.0004	0.022	0.23	–

(<sup>A</sup>) Cr, chromium; Ni, nickel; Mo, molybdenum; Cu, copper; C, carbon; Si, silicon; Mn, manganese; S, sulfur; P, phosphorus; N, nitrogen; Co, cobalt.

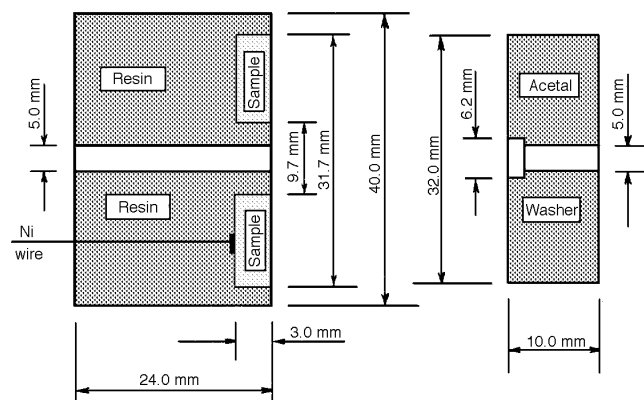


**FIGURE 1.** Configurations of the anode and crevice-forming washer in the remote crevice assembly.

done in a 34-L polypropylene tray at 21°C to 23°C. The water in the tray was quiescent, and it was refreshed continuously by a gravity feed and overflow system at a rate sufficient to replace the entire volume daily.

To separate the effect of microorganisms from that of water chemistry, a control water that had the same chemistry but few microorganisms was produced by pasteurizing the natural water at 80°C for 4 h. The water then was cooled to room temperature before use. Because of the large volume of control seawater used in this work (34 L at a time), additional preparation by filtration was not practical.

The remote crevice assembly technique physically separates the anode and cathode areas, enabling instantaneous determination of corrosion rates by measuring the current between the anode and the cathode using a zero-resistance ammeter. Each annular anode with a spot-welded nickel (Ni) wire was mounted in epoxy resin as shown in Figure 1. The solid acetal crevice washers (Figure 1) were attached to the mounted anodes using titanium fasteners, which were insulated from the anodes by heat-shrink tubing and tightened to an initial torque of 7.3 Nm. The assembly was retightened after 2 days and before the experiment.

To avoid corrosion on the Ni wire, the assembly

was immersed in the test solution so that the back side of the epoxy (from which the wire emerged) remained above the solution. The spot-welded wire on the anode was used both to secure the assembly to a wooden rack and to connect the anodes and cathodes. Two Ni wires spot welded to the top of each cathode panel served the same function. Cathode panels suspended from the Ni wires were immersed in the test solution to a depth of 104 mm  $\pm$  1 mm, producing a cathode-to-anode area ratio of 30:1. Suspending the cathode panels in this way left the spot weld far enough (40 mm to 45 mm) above the water surface that galvanic corrosion between the cathode and Ni wire could be avoided without painting the junction. The tradeoff was the introduction of an air-water interface on the surface of the cathode panel.

Two sets of experiments using triplicate samples (one for UNS N08367) were performed. The first set was used to study the effect of biofilms on the initiation and propagation of crevice corrosion. In this set, crevice corrosion on the anodes was initiated naturally. The second set was used to investigate the effect of biofilms on propagation alone using preinitiated anodes and pre-nobled cathodes. Before connecting the anodes and cathodes in the second set, corrosion on the anodes was initiated galvanostatically at 40 mA for 30 min.

In a separate test, six anodes of UNS S31603 were subjected to the above galvanostatic initiation procedure. Corrosion for each of the six anodes initiated in a narrow annular ring around the outer edge. The percentages of area corroded under the washer (PAC) were 13%  $\pm$  2% for the six anodes. The weight loss estimated using Faraday's law was 0.02 g, and the total charge passed was 72 coul for UNS S31603. This probably was an overestimation because some of the charge was consumed in breaking down the passive film. For other alloys, preinitiation resulted in a similar pattern of corrosion, but the reproducibility of the process was tested using multiple anodes only for UNS S31603. The cathodes were pre-nobled by immersing them in natural coastal seawater for ~ 3 weeks until the

potentials were near 400 mV<sub>SCE</sub>.

In the control tests, the water and cathodes were changed every 3 days. First, a clean tray with newly pasteurized water and clean cathodes was set up. The cathodes in this tray were allowed to equilibrate for 0.5 h. Next, the control anodes were disconnected from the old cathodes, transferred to the clean tray, and connected to the clean cathodes. The total elapsed time over which the anodes were disconnected electrically was < 30 s. The old cathodes and tray were immersed in fresh tap water at 60°C for 1 h and then air dried naturally and kept for future use. Two sets of control cathodes and two trays were recycled continuously in this manner.

Open-circuit potentials ( $E_{\text{corr}}$ ) were measured vs a saturated calomel reference electrode (SCE) using a Beckman RMS 3060<sup>†</sup> digital voltmeter with 22 M $\Omega$  impedance. The corrosion currents between the cathodes and anodes were measured using a zero-resistance ammeter (Thurston/Bell Associates Inc., Model AM 1000<sup>†</sup>). The time for crevice corrosion initiation for each anode was taken as the time when the corrosion current increased suddenly and remained above 0.

The cathodic polarization curves for the cathodes at the end of the preinitiated tests were measured using an EG&G PARC 273A<sup>†</sup> potentiostat computer controlled with PARC 352<sup>†</sup> software. The cathodes first were disconnected from the corresponding anodes. They then were allowed to sit under open-circuit conditions for 1 h to let the corrosion potentials recover to  $\sim 300$  mV<sub>SCE</sub>. The cathodes then were polarized from 100 mV greater than the  $E_{\text{corr}}$  value to  $-1,000$  mV<sub>SCE</sub> at a scan rate of 0.15 mV/s.

Weight losses for the anodes were determined to the nearest 0.01 g using a digital balance. Corroded anodes were cleaned by soap and brush, rinsed in milli-Q water, and air dried before weighing. The depths of attack for the anodes were measured using a needle-point dial gauge. Maximum and average depths of attack were recorded. The average depth was calculated from 10 to 34 measurements for each anode, depending on the extent of attack. The PAC for each anode also was measured.

Biofilm thickness on the cathode panels was measured using a stereomicroscope. Before the thickness was measured, a small portion of the biofilm was removed to reveal the bare cathode surface. The microscope then was focused sequentially on the biofilm surface and the bare cathode surface, to a precision of  $\pm 2.5$   $\mu\text{m}$ . Thus, the total uncertainty for each thickness measurement was  $\pm 5.0$   $\mu\text{m}$ . After the thickness measurement, the biofilm was fixed using 4% glutaraldehyde and stained using 0.1 mg/mL 4',6-diamidino-2-phenylindole (DAPI). Morphological types and

concentrations of bacteria visible in an undisturbed portion of the surface layers of the film then were determined using epifluorescence microscopy.

## RESULTS

### Crevice Corrosion Initiation

Table 2 gives initiation times for the first set of experiments, in which biofilms were allowed to form on the cathode panels and corrosion on the anodes was allowed to initiate naturally. Hereafter, "test anodes" refers to anodes connected to biofilmed cathodes in natural seawater and "control anodes" to anodes connected to cathodes in control water.

Neither the test nor the control anodes of UNS N08367 corroded for the entire test period. For the other alloys, the current densities for the test anodes rose at least one order of magnitude higher than those for the control anodes immediately after initiation. The t-test showed initiation times for the test anodes of UNS S31603 and S31725 were not statistically significantly different from those for the control anodes.

For UNS N08904, one test anode had no corrosion by the end of the experiments, and one control anode was lost. For the four remaining anodes that did corrode, the t-test showed that the initiation times for the test anodes were significantly shorter than those for the control anodes. However, when the third test anode, which did not initiate corrosion, was included and the initiation time for that anode was taken to be the total testing time, then the initiation times for the test anodes were not signifi-

**TABLE 2**  
*Effect of Biofilms on Crevice Corrosion Initiation Time in Naturally Initiated Tests<sup>(A)</sup>*

Alloy	Initiation Time (h)	
	Test	Control
UNS S31603	182	182
	155	420
	244	182
UNS S31725	244	267
	244	298
	267	182
UNS N08904	333	1,353
	517	1,400
	> 1,862 <sup>(B)</sup>	NA <sup>(C)</sup>
UNS N08367	> 1,862	> 1,862

<sup>(A)</sup> Remote crevice assembly, cathode-to-anode area ratio = 30, and initial torque = 7.3 Nm.

<sup>(B)</sup> No corrosion at the end of the test.

<sup>(C)</sup> NA, not available.

**TABLE 3**  
*Effect of Biofilms on Crevice Corrosion Propagation Parameters in Naturally Initiated Tests<sup>(A)</sup>*

Alloy	Weight Loss (g)		PAC <sup>(B)</sup> (%)		Maximum Depth (mm)		Average Depth (mm)	
	Test	Control	Test	Control	Test	Control	Test	Control
UNS S31603	1.11	0.09	80	55	1.52	0.14	0.39	0.04
	1.16	< 0.01	80	< 1	1.27	< 0.01	0.47	< 0.01
	1.04	0.08	90	55	0.81	0.14	0.36	0.04
UNS S31725	0.97	0.05	80	60	1.98	0.09	0.34	0.04
	0.70	0.04	65	35	0.94	0.13	0.30	0.03
	0.83	0.01	75	50	1.17	0.05	0.29	0.02
UNS N08904	0.53	< 0.01	80	< 1	1.30	< 0.01	0.21	< 0.01
	0.55	< 0.01	80	< 1	0.94	< 0.01	0.17	< 0.01
	0	NA <sup>(C)</sup>	0	NA	NA	NA	0	NA
UNS N08367	0	0	0	0	0	0	0	0

<sup>(A)</sup> Conditions were as in Table 2.

<sup>(B)</sup> PAC, percentage of area corroded under the washer.

<sup>(C)</sup> NA, not available.

cantly less than those for the controls.

### Crevice Corrosion Propagation

Table 3 gives weight losses, PAC values, and maximum and average depths of attack for the anodes on which crevice corrosion initiated naturally (the first set). Neither the test nor control anodes of UNS N08367 had corroded by the end of the tests. For the other alloys, crevice corrosion propagation for the test anodes was much faster than that for the control anodes. Weight losses of all corroded test anodes were one to two orders of magnitude more than those of the control anodes. For UNS S31603 and S31725, PAC values for the test anodes were generally much larger than those for the control anodes. PAC values for the corroded test anodes of UNS N08904 were 80%, while PAC values for control anodes of UNS N08904 were < 1%. For all corroded anodes, maximum and average depths of attack in natural seawater were one to two orders of magnitude larger than those in control seawater. For UNS S31603, S31725, and the four anodes of N08904 that did corrode, the differences between propagation rates in natural and control seawaters were significant statistically, while for UNS N08904 the differences were not significant statistically if all five anodes were included.

Table 4 gives weight losses, PAC values, and maximum and average depths of attack for the anodes on which crevice corrosion was preinitiated. After the UNS N08367 anodes were connected to the biofilmed and bare cathodes, corrosion currents decreased to 0 and corrosion stopped within 12 h. Corrosion did not initiate again during the test. For the other alloys, weight losses and maximum and

average depths of attack for all test anodes were one to two orders of magnitude larger than those of all control anodes. PAC values for all test anodes of UNS S31603, S31725, and N08904 generally were larger than those for the control anodes. The differences between propagation in natural and control seawaters were significant statistically.

Figures 2 through 4 show the measured corrosion current densities for the anodes in tests of natural initiation. In those figures, the current density-vs-time curves for the control anodes were smoothed statistically using three-point averaging.<sup>15</sup> Smoothing was desirable because of the large transient fluctuations introduced when cathodes were changed. Because the logarithmic scale was used, no data are shown until the time at which corrosion actually initiated. Figures 2 and 3 show that the current densities for the test anodes of UNS S31603 and S31725 were at least one and a half orders of magnitude higher than those for the control anodes of the same alloys. The current densities for the corroded anodes of UNS N08904 in natural seawater (Figure 4) were nearly three orders of magnitude higher than those in control seawater. Figure 5 shows typical  $E_{\text{corr}}$ -vs-time records for test and control cathode-anode couples of UNS S31725.  $E_{\text{corr}}$  for the test couple first reached 100 mV<sub>SCE</sub>, then decreased to  $\leq -50$  mV<sub>SCE</sub> after initiation. The process of changing the control water and cathode caused the fluctuations in  $E_{\text{corr}}$  for the control couple.

Figures 6 through 8 show the measured current densities after the initiation procedure for the anodes of UNS S31603, S31725, and N08904 in the preinitiated experiments. After reaching stable values, current densities for the test anodes of UNS



**TABLE 4**  
*Effect of Biofilms on Crevice Corrosion Propagation Parameters in Preinitiated Tests<sup>(A)</sup>*

Alloy	Weight Loss (g)		PAC (%)		Maximum Depth (mm)		Average Depth (mm)	
	Test	Control	Test	Control	Test	Control	Test	Control
UNS S31603	0.88	< 0.01	90	53	1.61	< 0.01	0.46	< 0.01
	0.79	< 0.01	67	65	1.28	< 0.01	0.44	< 0.01
	0.87	0.05	73	38	1.75	0.64	0.50	0.11
UNS S31725	0.60	< 0.01	85	25	1.40	< 0.01	0.22	< 0.01
	0.66	< 0.01	93	5	1.30	< 0.01	0.23	< 0.01
	0.58	< 0.01	80	20	1.78	< 0.01	0.24	< 0.01
UNS N08904	0.51	< 0.01	65	< 1	1.16	< 0.01	0.26	< 0.01
	0.67	< 0.01	75	< 1	1.35	< 0.01	0.27	< 0.01
	0.60	< 0.01	95	< 1	1.04	< 0.01	0.19	< 0.01
UNS N08367	< 0.01	< 0.01	< 1	< 1	< 0.01	< 0.01	< 0.01	< 0.01

<sup>(A)</sup> Conditions were as in Table 2.

S31603 and S31725 were two orders of magnitude higher than for the controls. The current densities for test anodes of UNS N08904 were two and a half orders of magnitude higher than that for one control anode, while corrosion on the other two control anodes stopped, giving no measured current.

Figure 9 shows typical potential-vs-time curves for one test couple and one control couple of UNS S31725. After the corrosion rates of the test and control samples became steady,  $E_{\text{corr}}$  values stayed around  $-50 \text{ mV}_{\text{SCE}}$  and  $-200 \text{ mV}_{\text{SCE}}$ , respectively.

Figure 10 shows cathodic polarization curves for the cathodes of UNS S31725 at the end of the preinitiated experiments (curves for UNS S31603 and N08904 were similar and are not shown). At any given potential above  $-600 \text{ mV}_{\text{SCE}}$ , current densities for the cathodes on which corrosion was initiated naturally were higher than those for controls.

The curves for biofilmed cathodes in Figure 10 did not show the depletion peak often observed for ennobled SS under continuous open-circuit conditions.<sup>16</sup> The biofilmed cathodes in the present work, however, were connected to corroding anodes and they covered with calcareous deposits in addition to biofilms by the end of the experiments. Also, because of the influence of the corroding anodes,  $E_{\text{corr}}$  for the anode-cathode couples was shifted to  $-50 \text{ mV}_{\text{SCE}}$ , and cathodic species, such as peroxide,<sup>16</sup> were consumed continuously. These reasons should be sufficient to account for the differences between the cathodic curves measured here and those for SS ennobled under open-circuit conditions.<sup>16</sup>

### Biofilm Analysis

Biofilm thicknesses on the test cathodes in natural seawater are listed in Table 5. These films were many layers of organisms thick, and only the

outermost layer could be observed in the microscope. In contrast, biofilms on the control cathodes were  $< 5 \mu\text{m}$  thick, and they provided less than complete coverage, with bare metal visible between the organisms in many places. Coccoidal, rod, and filamentous bacteria were observed on the biofilmed cathodes in natural seawater. Bacterial densities observable in the outer layers of the biofilmed cathodes were  $2.1$  to  $2.7 \times 10^6$  cells/cm<sup>2</sup> in the naturally initiated experiments and  $1.0$  to  $10.9 \times 10^6$  cells/cm<sup>2</sup> in the preinitiated tests. On the control cathodes, bacteria were scattered at densities of  $1.5$  to  $5.0 \times 10^5$  cells/cm<sup>2</sup>.

Biofilm thickness was more important than the bacteria count because the thickness was more representative of the total biomass, whereas the count reflected only those bacteria observable in the outer layers of the biofilm. Further, the process of immersing the control cathodes in fresh water at  $60^\circ\text{C}$  for 1 h and air drying for 3 days killed most bacteria on them. Although the bacteria that were counted on the control cathodes still may have affected the electrochemistry on the surface, the combination of incomplete biofilm coverage and mostly dead bacteria effectively eliminated the ennoblement of  $E_{\text{corr}}$  and greatly reduced the cathodic reaction acceleration that accompanies ennoblement.

## DISCUSSION

### Crevice Corrosion Initiation Time

Theoretically, any shift of  $E_{\text{corr}}$  in the noble direction should increase the initiation probability and decrease the initiation time. Therefore, the ennoblement of  $E_{\text{corr}}$  by biofilms should reduce the initiation time.

This tended to be true only for UNS N08904 in

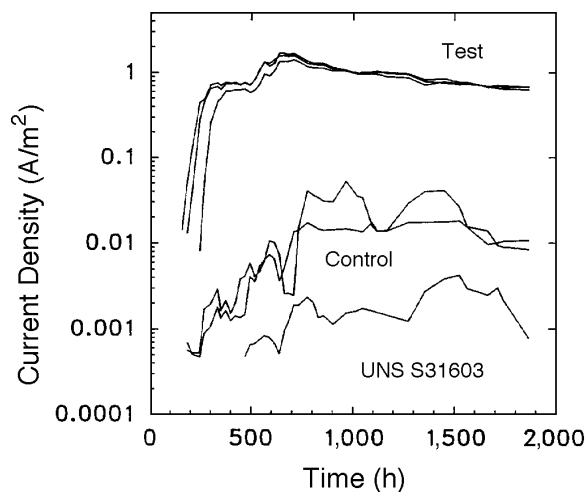


**FIGURE 2.** Remote crevice assembly data of current density vs time for the UNS S31603 anodes in naturally initiated tests.

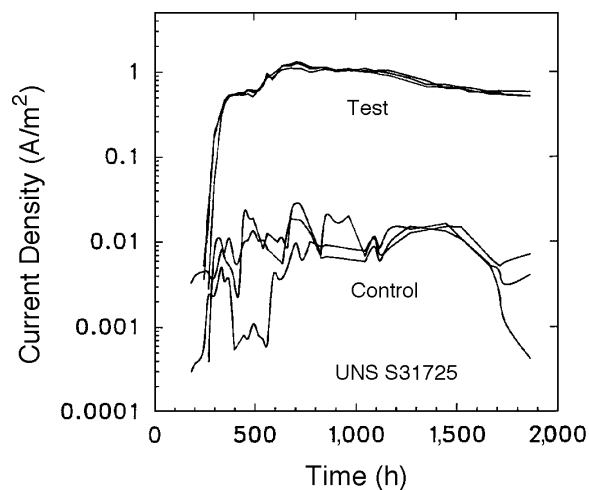


**FIGURE 3.** Remote crevice assembly data of current density vs time for UNS S31725 anodes in naturally initiated tests.

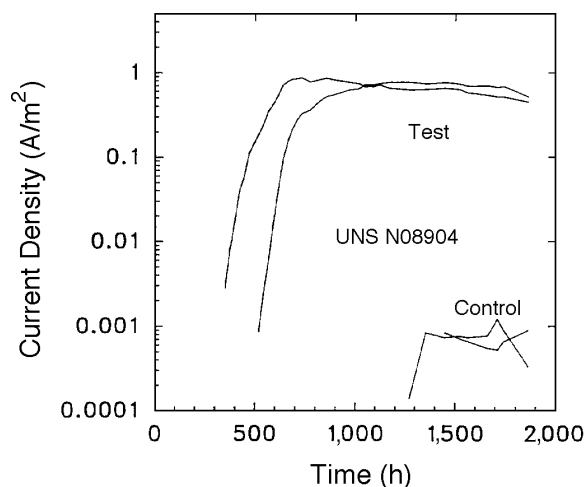


**FIGURE 4.** Remote crevice assembly data of current density vs time for UNS N08904 anodes in naturally initiated tests.

the present work. Considering the four corroded anodes of UNS N08904, there was a trend toward a decrease in initiation time for the test anodes compared to the control anodes. Although the t-test showed this decrease was significant statistically, that judgment was based on only two anodes each, and the significance disappeared when the uncorroded test anode was included. For UNS S31603 and S31725, on which corrosion initiated for all anodes, biofilms did not affect initiation times significantly.

The uncertainty in these results was consistent with previous results by Zhang and Dexter,<sup>9</sup> Kain and Lee,<sup>11</sup> and Valen.<sup>12</sup> Using a less effective control than in the present work, Zhang and Dexter found biofilms

tended to decrease initiation times for UNS S31603, S31725, and N08904.<sup>9</sup> Kain and Lee observed that initiation times for UNS S31603 in natural and artificial seawater did not differ, while the initiation time for UNS N08904 in natural seawater was only 10% that in artificial seawater.<sup>11</sup> Valen measured longer initiation times for test samples of UNS S31603 than for a control sample, which probably was due to the much larger cathode-to-anode area ratio (2,000:1) for the control sample than those (5:1, 20:1, and 100:1) for the test samples.<sup>12</sup> However, no statistical analysis was made by those authors. Gallagher, et al., did not determine initiation time.<sup>14</sup>

Thus, although the present data seemed to show biofilms decreased the initiation times for the corroded UNS N08904 anodes and did not affect the initiation times for UNS S31603 and S31725, it was not possible to make a statistically valid conclusion about the general effect of biofilms on initiation times because of the small number of samples tested. More samples must be tested to settle this issue, and future work will address this area.

In the present work, corrosion did not initiate at the air-water interface on the cathodes. This was understandable for the controls because they were changed frequently and because the salts on them were removed during their immersion in fresh water at 60°C for 1 h. For the cathodes in tests of natural initiation, this probably was due to corrosion initiation on the anodes, which provided cathodic protection for the corresponding cathodes.

### Crevice Corrosion Propagation

Among the five propagation parameters measured in these tests (weight loss, PAC, average and maximum depths of attack, and current density),

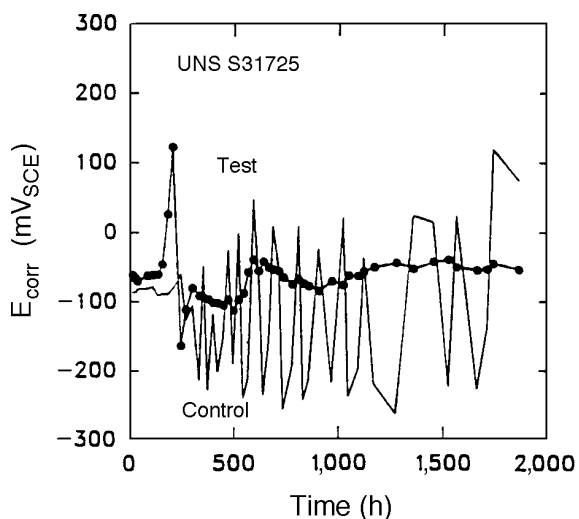


**FIGURE 5.**  $E_{corr}$  vs time for UNS S31725 samples in naturally initiated tests.

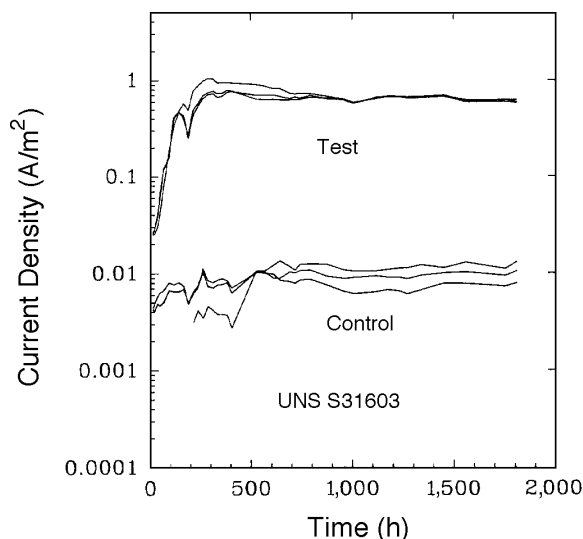


**FIGURE 6.** Remote crevice assembly data of current density vs time for UNS S31603 anodes in preinitiated tests.

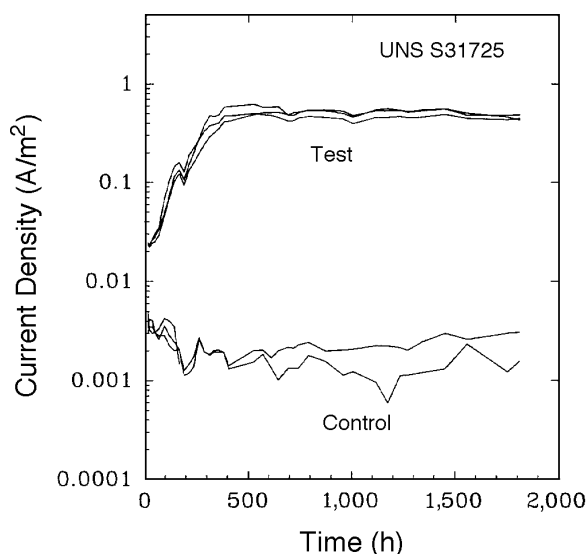


**FIGURE 7.** Remote crevice assembly data of current density vs time for UNS S31725 anodes in preinitiated tests.

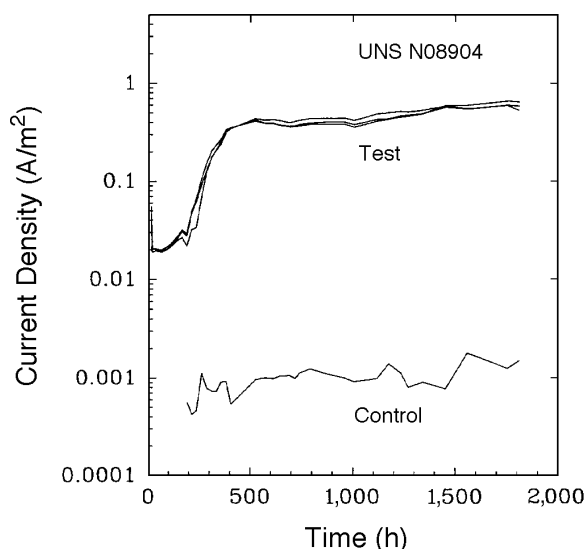


**FIGURE 8.** Remote crevice assembly data of current density vs time for UNS N08904 anodes in preinitiated tests.

PAC was the least significant in the practical sense. Weight loss (or current density) and depth of attack are more closely related to the lifetime of a structural component than PAC, which measures only the lateral extent of attack.

In contrast to the case of initiation, biofilms increased current densities for crevice corrosion propagation by one to three orders of magnitude for UNS S31603, S31725, and N08904 (Figures 2 through 4 and 6 through 8). This increase resulted in large increases in weight loss as well as in maximum and average depths of attack for these alloys (Tables

3 and 4).

Data for UNS S31603 were in good agreement with the results of Valen, who showed that the current densities for UNS S31603 samples in natural seawater were one to two orders of magnitude higher than in artificial seawater.<sup>12</sup> Gallagher, et al., found almost no crevice corrosion for UNS S31603 in artificial seawater.<sup>14</sup> In the present results (Tables 3 and 4), there was some attack on the control anodes of UNS S31603. PAC values for the control anodes were much larger than those found by Gallagher, et al., but the depths of attack were very shallow. The



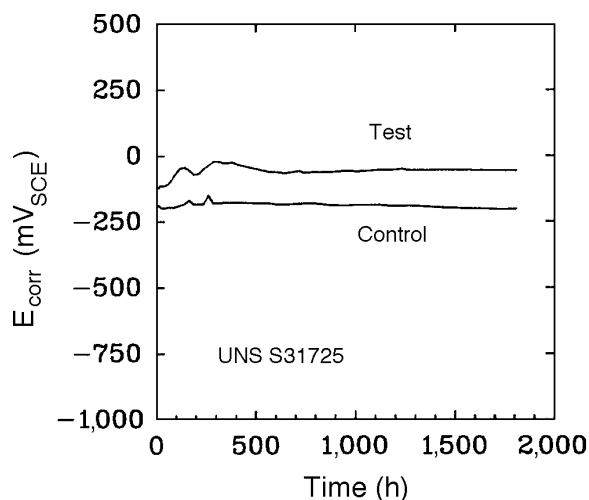


FIGURE 9.  $E_{corr}$  vs time for UNS S31725 samples in preinitiated tests.

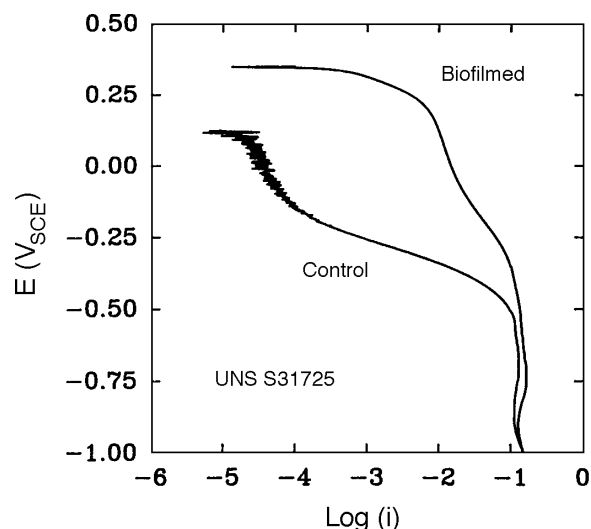


FIGURE 10. Cathodic polarization curves for the UNS S31725 cathodes at the end of the preinitiated tests.

TABLE 5

Biofilm Thicknesses on Cathode Panels

Alloy	Film Thickness on Biofilmed Cathodes <sup>(A)</sup>	
	Naturally Initiated Tests	Preinitiated Tests
UNS S31603	61 $\mu\text{m} \pm 19 \mu\text{m}$	45 $\mu\text{m} \pm 15 \mu\text{m}$
UNS S31725	46 $\mu\text{m} \pm 16 \mu\text{m}$	43 $\mu\text{m} \pm 17 \mu\text{m}$
UNS N08904	47 $\mu\text{m} \pm 16 \mu\text{m}$	41 $\mu\text{m} \pm 20 \mu\text{m}$
UNS N08367	27 $\mu\text{m} \pm 6 \mu\text{m}^{(B)}$	20 $\mu\text{m} \pm 7 \mu\text{m}^{(B)}$

<sup>(A)</sup> Average of six measurements on one cathode for each alloy.

<sup>(B)</sup> No calcareous deposits were in the films; the other cathodes had a mixture of calcareous deposits and bacteria.

Gallagher, et al., artificial seawater control was probably less corrosive than the pasteurized seawater used in this work. The reason for the difference was unknown, but it probably was related to the fact that the chemistry of the pasteurized water was different from that of artificial seawater.

The control anodes for S31603 and S31725 in this work had less corrosion than those reported in the previous paper of Zhang and Dexter,<sup>9</sup> because the control method used here was more effective. Thus, the combination of pasteurizing the seawater and periodically changing the cathodes after heating them in fresh water maintained control conditions better and was more convenient than using filtered seawater alone in long-term tests.

The data in Tables 3 and 4 and Figures 4 and 8 showed propagation rates for UNS N08904 in natural seawater were nearly three orders of magnitude higher than those in control seawater. It was hard to compare these data for UNS N08904 with those from Gallagher, et al.,<sup>14</sup> because Gallagher did not give

specific values for depths of attack and PAC. However, it seemed that the results for UNS N08904 here were consistent with results of Gallagher, et al. Results here also agreed with those of Zhang and Dexter<sup>9</sup> and Kain and Lee.<sup>11</sup>

According to the mixed potential theory, total anodic current must be equal to total cathodic current during an electrochemical reaction. The steady potentials for the test and control samples of UNS S31725 were  $-50 \text{ mV}_{\text{SCE}}$  and  $-200 \text{ mV}_{\text{SCE}}$ , respectively (Figure 9). At these two potentials, the current densities for the biofilmed and control cathodes of UNS S31725 in the cathodic polarization curves of Figure 10 were  $2.4 \times 10^{-2} \text{ A/m}^2$  and  $2.23 \times 10^{-4} \text{ A/m}^2$ , respectively. Because of the 30:1 cathode-to-anode area ratio, these current densities would become  $0.72 \text{ A/m}^2$  and  $0.0067 \text{ A/m}^2$  on anodes connected to them at those potentials. Current densities for the test anodes in Figure 7 were  $\sim 0.7 \text{ A/m}^2$ , which was in excellent agreement with the  $0.72 \text{ A/m}^2$  calculated above. Current densities for the control anodes in Figure 7 were  $\sim 0.003 \text{ A/m}^2$ , which was of the same order of magnitude as the  $0.0067 \text{ A/m}^2$  estimated above. Therefore, the anodic current densities calculated from cathodic polarization curves were in good agreement with those measured using a zero-resistance ammeter. These results, along with those for UNS S31603 and N08904, are listed in Table 6. Therefore, it was concluded that the increased propagation in the presence of biofilms was caused by an increase in the kinetics of the cathodic reaction by biofilms. The increase of the cathodic reaction by biofilms also has been reported by others.<sup>3,6,17-18</sup>

Theoretical weight losses for the anodes were

**TABLE 6**  
Calculated ( $i_c$ ) and Measured ( $i_m$ ) Current Densities ( $A/m^2$ )  
for Anodes in the Preinitiated Tests

	Natural			Control		
	$i_m$	$i_c$	Diff. (%) <sup>(A)</sup>	$i_m$	$i_c$	Diff. (%)
UNS S31603	0.8	0.77	-3.7	0.009	0.0099	10
UNS S31725	0.7	0.72	2.8	0.003	0.0067	123
UNS N08904	0.8	1.17	46.3	0.001	0.0021	110

<sup>(A)</sup> Diff. (%) =  $(i_c/i_m - 1) \times 100$ .

**TABLE 7**  
Calculated ( $W_c$ ) and Measured ( $W_m$ ) Weight Losses (g)  
for Anodes in the Naturally Initiated Tests

	Test			Control		
	$W_m$	$W_c$	Diff. (%) <sup>(A)</sup>	$W_m$	$W_c$	Diff. (%)
UNS S31603	1.11	0.981	-11.6	0.09	0.021	-76.6
	1.16	1.033	-10.9	< 0.01	0.002	NC <sup>(B)</sup>
	1.04	0.908	-12.7	0.08	0.022	-72.5
UNS S31725	0.97	0.822	-15.3	0.05	0.021	-58.0
	0.70	0.789	12.7	0.04	0.016	-60.0
	0.83	0.799	3.7	0.01	0.022	120.0
UNS N08904	0.53	0.567	7.0	NA <sup>(C)</sup>	NA	NA
	0	0	NC	< 0.01	0.0004	NC
	0.55	0.500	-9.1	< 0.01	0.0002	NC

<sup>(A)</sup> Diff. (%) =  $(W_c/W_m - 1) \times 100$ .

<sup>(B)</sup> NC, not calculable.

<sup>(C)</sup> NA, not available.

calculated using the measured current densities and Faraday's law:

$$W_T = k_a i t \quad k_a = \frac{W_a}{F n_a} \quad (1)$$

where  $W_T$  represents theoretical weight loss;  $i$  is the corrosion current density; and  $k_a$ ,  $W_a$ , and  $n_a$  are the electrochemical equivalent, atomic weight, and valence number for each alloy.  $n_a$  and  $W_a$  were calculated as follows:

$$n_a = \sum n_i f_i \quad (2)$$

$$W_a = \sum w_i f_i \quad (3)$$

where  $f_i$ ,  $w_i$ , and  $n_i$  are the mole fraction, atomic weight, and valence numbers for individual elements in the alloy, assuming that all elements were corroded in proportion to their mole fraction. The percentages by weight shown in Table 1 were converted to  $f_i$  by dividing  $w_i$  by the total molal amount of all elements for a sample of 100 g.  $w_i$  and

$n_i$  were taken from the *CRC Handbook of Chemistry and Physics*.<sup>19</sup> The calculated weight losses ( $W_c$ ) shown in Tables 7 and 8 are in good agreement with the corresponding measured weight losses ( $W_m$ ). For some control anodes, the percentage differences between  $W_c$  and  $W_m$  were large. However, the differences were insignificant because the absolute values of the measured weight losses for all control anodes were very small.

For UNS N08367, crevice corrosion did not initiate in natural or control seawater in naturally initiated tests. Corrosion stopped for the UNS N08367 anodes that had preinitiated crevice corrosion after they were connected to biofilmed and bare cathodes. Therefore, biofilms did not affect crevice corrosion of the highly resistant 6% Mo alloy, UNS N08367, in these 2-month tests. Biofilms did increase the crevice corrosion propagation rate for the intermediately resistant alloys, UNS N08904 and S31703, and for the low-resistance alloy, UNS S31603. However, the increases in propagation attributable to biofilms for UNS N08904 and S31703 was five to 10 times higher than that for UNS S31603. This partially was due to the fact that UNS

**TABLE 8**  
 $W_c$  and  $W_m$  (g) for Anodes in the Preinitiated Tests

	Test			Control		
	$W_m$	$W_c$	Diff. (%)	$W_m$	$W_c$	% Diff.
UNS S31603	0.88	0.818	-7.0	< 0.01	0.009	NC <sup>(A)</sup>
	0.79	0.726	-8.1	< 0.01	0.01	NC
	0.87	0.736	-15.4	0.05	0.012	-76
UNS S31725	0.60	0.507	-15.5	< 0.01	0.003	NC
	0.66	0.541	-18.0	< 0.01	0.002	NC
	0.58	0.469	-19.1	< 0.01	0.0004	NC
UNS N08904	0.51	0.448	-12.2	< 0.01	0	NC
	0.67	0.452	-32.5	< 0.01	0.001	NC
	0.60	0.471	-21.5	< 0.01	0	NC

<sup>(A)</sup> NC, not calculable.

S31603 corrodes readily in saline solutions whether biofilms are present or not. These results agreed with the previous suggestion that the influence of biofilms on crevice corrosion should be most significant on alloys that have intermediate resistance.<sup>9</sup>

## CONCLUSIONS

- ❖ Biofilms did not affect initiation times for UNS S31603 and S31725 significantly in this work. For all samples of UNS N08904 that initiated corrosion, biofilms decreased the initiation time significantly. However, a larger number of samples will be needed before a general conclusion can be reached about the effect of biofilms on crevice corrosion initiation time for these alloys.
- ❖ Biofilms increased the propagation rate for crevice corrosion on UNS S31603, S31725, and N08904 by one to three orders of magnitude. The increase of the propagation rate was due to the increase in kinetics of the cathodic reaction by the biofilms.
- ❖ The theoretical weight losses calculated using the measured current densities and Faraday's law were in good agreement with the measured weight losses.
- ❖ A combination of pasteurization of control water and periodic change of the cathode panels after heating them in fresh water provided a more effective and practical control condition than treatment of the water alone for these experiments, which required large volumes of water and long exposure times.

## ACKNOWLEDGMENTS

This research was supported by the National Oceanic and Atmospheric Administration Office of Sea Grant, U.S. Department of Commerce, under grant no. NA16RG0162-01. The authors acknowledge

the donation of samples by Allegheny Ludlum Steel Corp.

## REFERENCES

1. A. Mollica, A. Trevis, "Correlation Entre la Formation de la Pellicule Primaire et la Modification de la Cathodique sur des Aciers Lnoxydables Experimentes en Eau de Mer aux Vitesses de 0.3 a 5.2 m/s," Proc. 4th Int. Cong. Marine Corrosion and Fouling, Antibes-Juan-les Pins, France, June 1976, p. 351.
2. S.C. Dexter, *Biofouling* 7 (1993): p. 97.
3. R. Holthe, E. Bardal, P.O. Gartland, "Time Dependence of Cathodic Properties of Stainless Steels, Titanium, Platinum, and 90/10 CuNi in Seawater," CORROSION/88, paper no. 393 (Houston, TX: NACE, 1988).
4. R. Johnsen, E. Bardal, *Corrosion* 41 (1985): p. 296.
5. S.C. Dexter, G.Y. Gao, *Corrosion* 44 (1988): p. 717.
6. V. Scotto, R. Di Cintio, G. Marcenaro, *Corros. Sci.* 25 (1985): p. 185.
7. S.C. Dexter, H.-J. Zhang, "Effect of Biofilms on Corrosion Potential of Stainless Alloys in Estuarine Waters," Proc. 11th Int. Corrosion Cong., held in Florence, Italy, April 1990, p. 4.333.
8. S.C. Dexter, H.-J. Zhang, "Effect of Biofilms, Sunlight, and Salinity on Corrosion Potential and Corrosion Initiation," Proc. Microbiologically Influenced Corros. and Biodegradation, eds. N.J. Dowling, M.W. Mittelman, J.C. Danko, held in Knoxville, Tennessee, October 1990, p. 8-1.
9. H.-J. Zhang, S.C. Dexter, "Effect of Marine Biofilms on Crevice Corrosion of Stainless Alloys," CORROSION/92, paper no. 400 (Houston, TX: NACE, 1992).
10. S.C. Dexter, K.E. Lucas, G.Y. Gao, "The Role of Marine Bacteria in Crevice Corrosion Initiation," Proc. Biologically Induced Corrosion, ed. S.C. Dexter (Houston, TX: NACE, 1986), p. 144.
11. R.M. Kain, T.S. Lee, in *Laboratory Corrosion Tests and Standards*, STM STP 866, eds. G.S. Haynes, R. Baboian (Philadelphia, PA: ASTM, 1985), p. 299.
12. S. Valen, (Master's thesis, Norwegian Institute of Technology, 1986).
13. A. Mollica, A. Trevis, E. Traverso, G. Ventura, G. DeCarolis, R. Dellepiane, *Corrosion* 44 (1988): p. 194.
14. P. Gallagher, R.E. Malpas, E.B. Shone, *Brit. Corros. J.* 23 (1988): p. 229.
15. C. Chatfield, *The Analysis of Time Series* (London, England: Chapman and Hall, 1984), p. 143.
16. H.-J. Zhang, "The Effect of Biofilms on Localized Corrosion of Stainless Alloys" (Ph.D. diss., University of Delaware, 1993), p. 74.
17. V. Scotto, "Electrochemical Studies of Biocorrosion of Stainless Steels in Seawater," Proc. Electric Power Research Institute Workshop on Microbial-Induced Corrosion, EPRI ER-6345 (Palo Alto, CA: EPRI, 1989), p. B-1.
18. S. Motoda, Y. Suzuki, T. Shinohara, S. Tsujikawa, *Corros. Sci.* 31 (1990): p. 515.
19. CRC Handbook of Chemistry and Physics, 74th ed., ed. D.R. Lide (Boca Raton, FL: CRC, 1993), p. 1.